Morphology controlled synthesis of $MnCO_3$-RGO materials and their supercapacitor applications

*Milan Jana,[a,b] Pranab Samanta,[a,b] Naresh Chandra Murmu,[a,b] and Tapas Kuila,[a,b] **

[a] Surface Engineering & Tribology Division, Council of Scientific and Industrial Research-Central Mechanical Engineering Research Institute, Durgapur -713209, India

[b] Academy of Scientific and Innovative Research (AcSIR), CSIR-CMERI Campus, Durgapur, 713209, India

---

* Corresponding author. Tel.: +91-9647205077; Fax: 91-343-2548204

E-mail address: tkuila@gmail.com (Tapas Kuila)

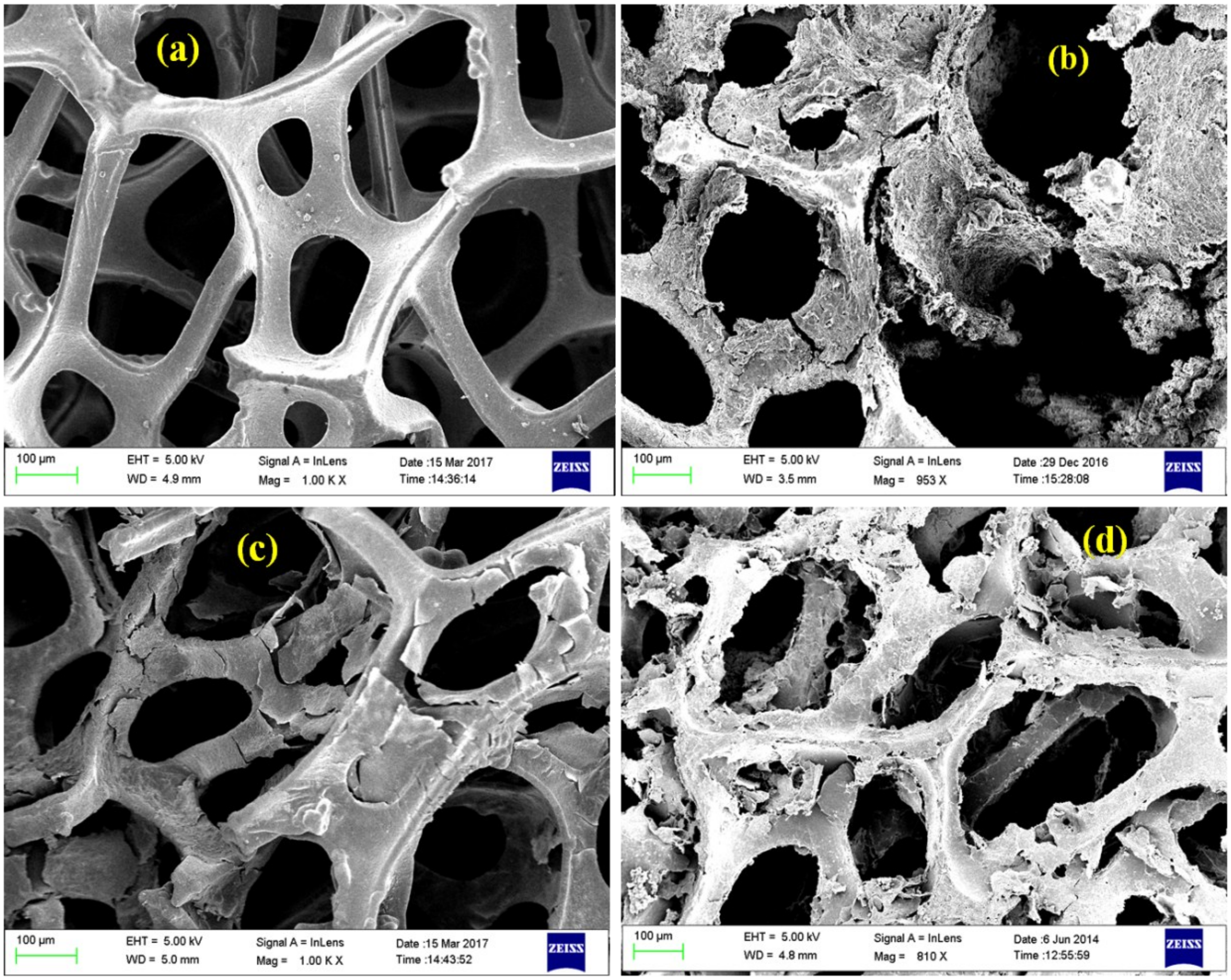

Fig. S1. FE-SEM images of (a) bare NF, (b) CMRGO, (c) OMRGO and (d) TMRGO deposited NF.

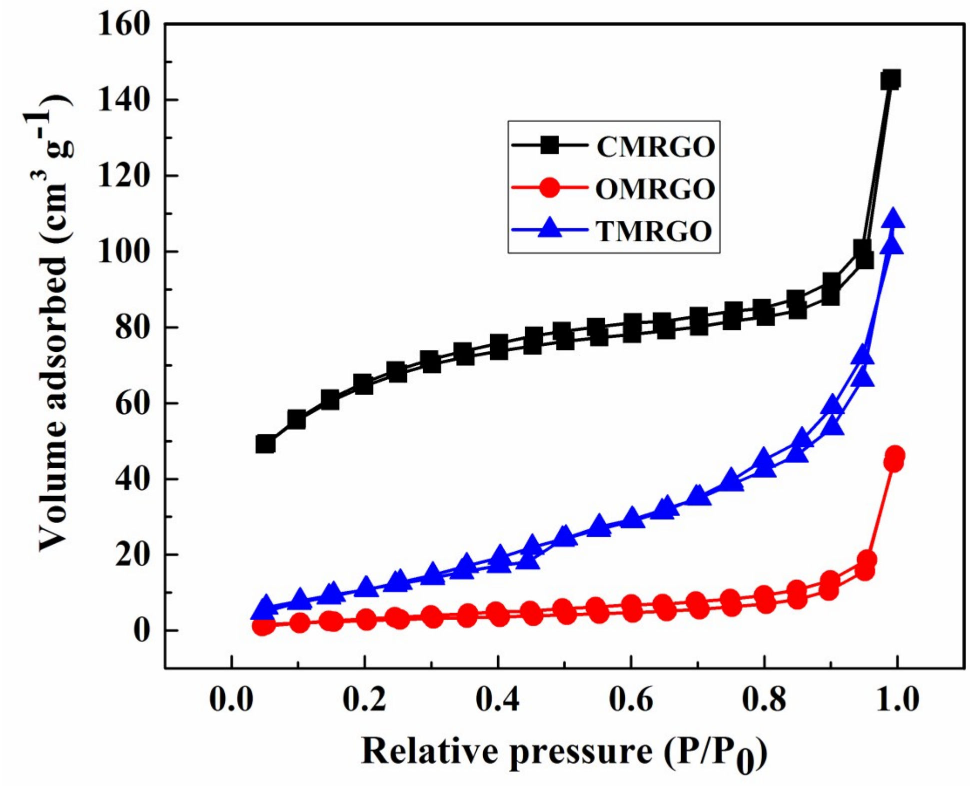

Fig. S2. N_2 adsorption-desorption isotherms.

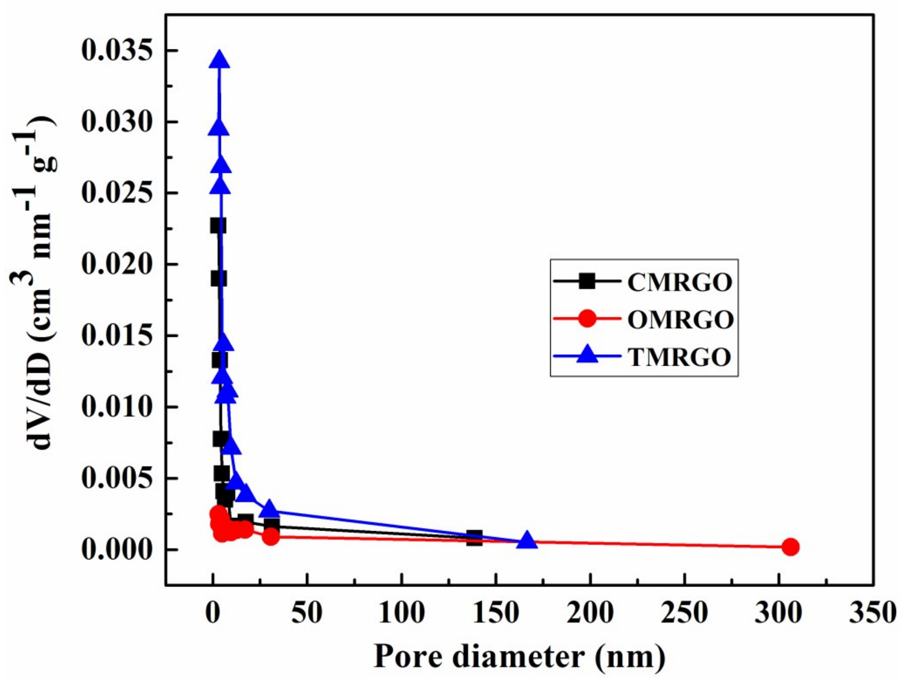

Fig. S3. BJH pore size distribution profile.

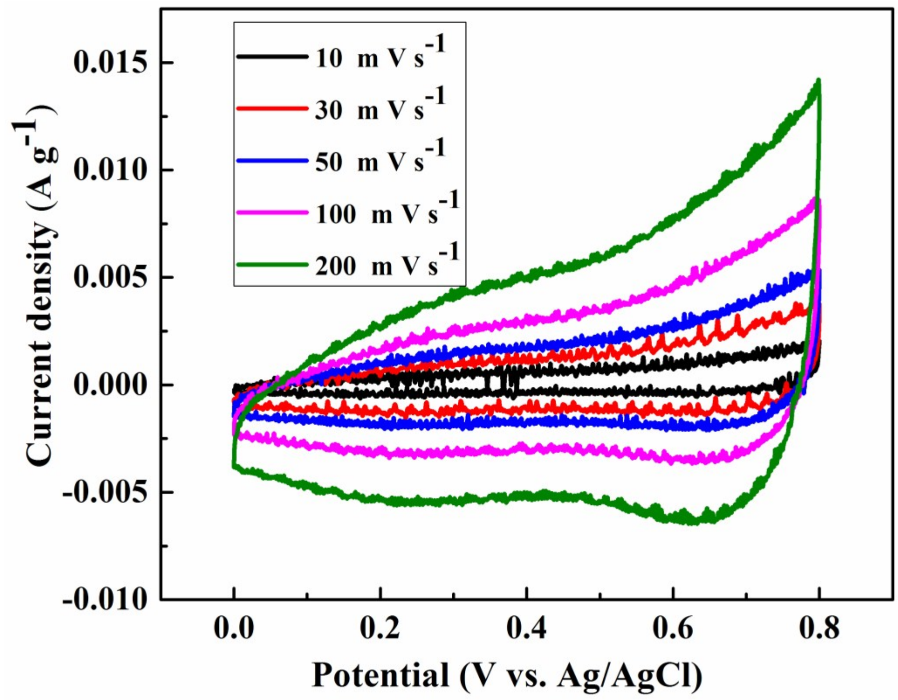

Fig. S4. CV curves of bare NF.

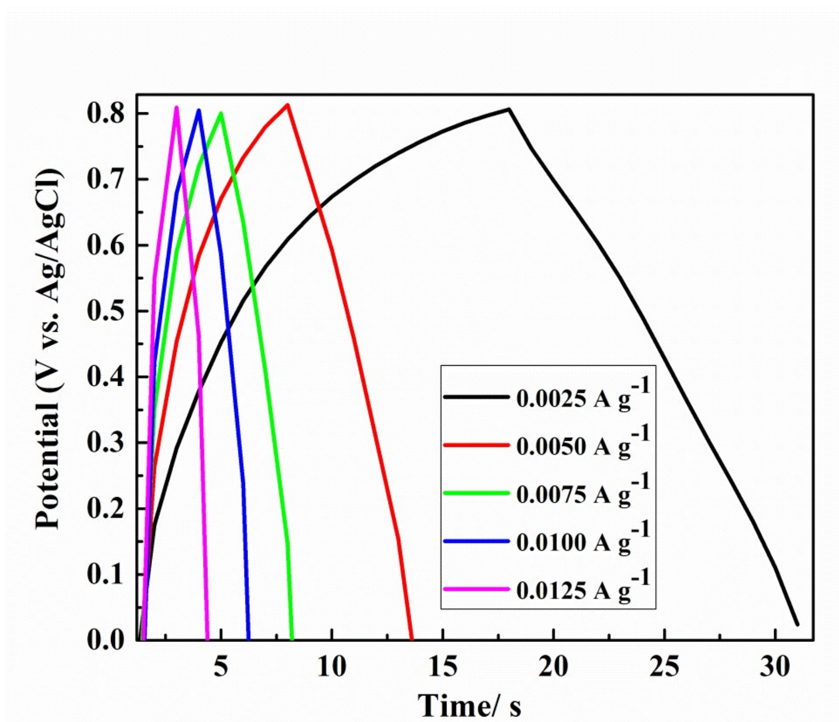

Fig. S5. GCD curves of bare NF.

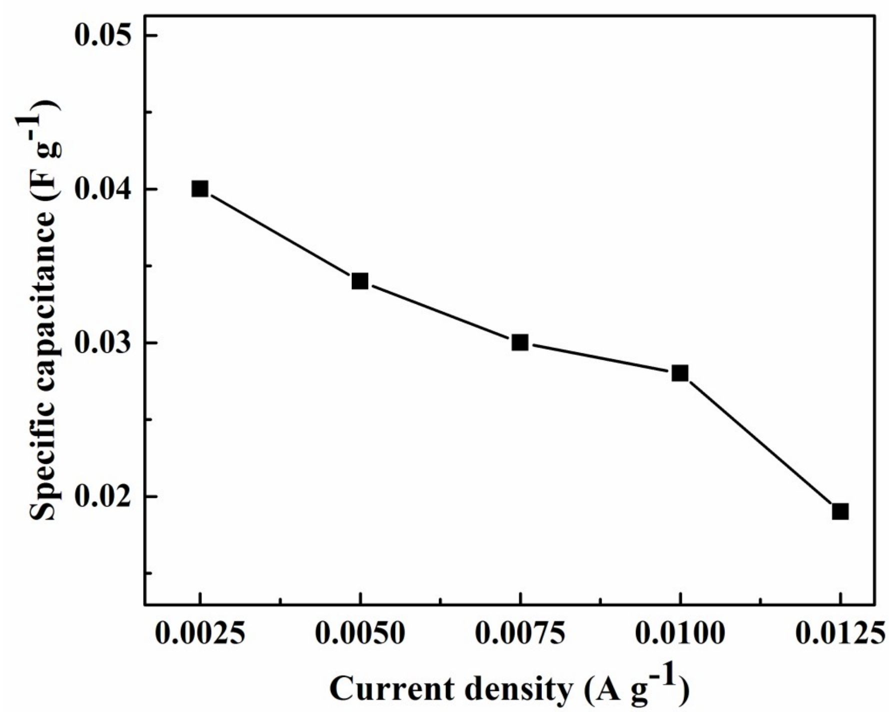

Fig. S6. SC vs. current density of NF.

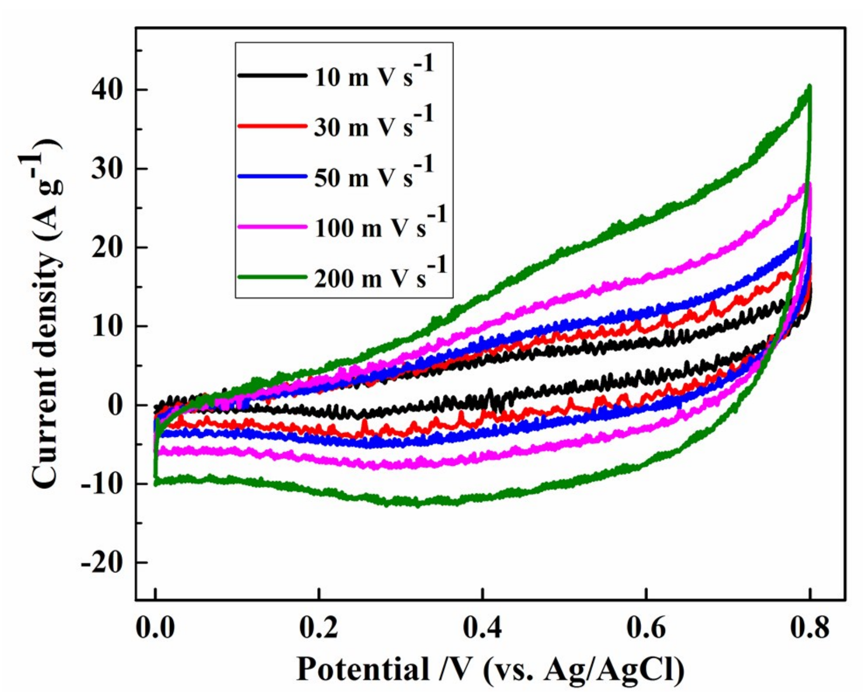

Fig. S7. CV curves of pure $MnCO_3$.

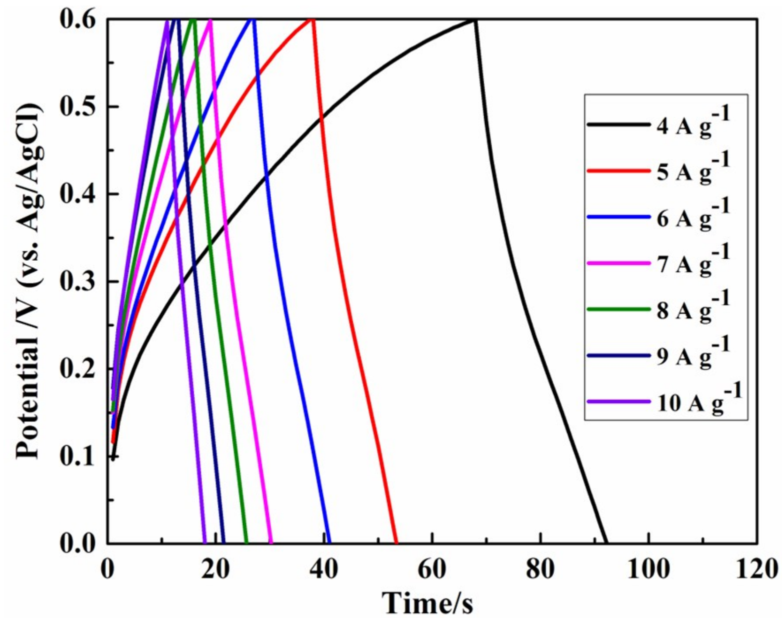

Fig. S8. GCD curves of pure $MnCO_3$.

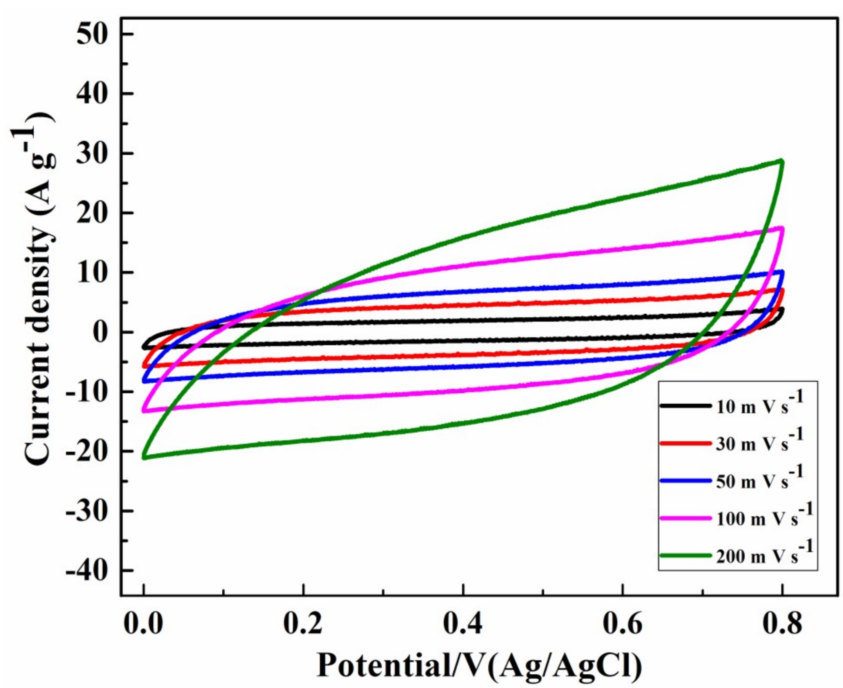

Fig. S9. CV curves of RGO.

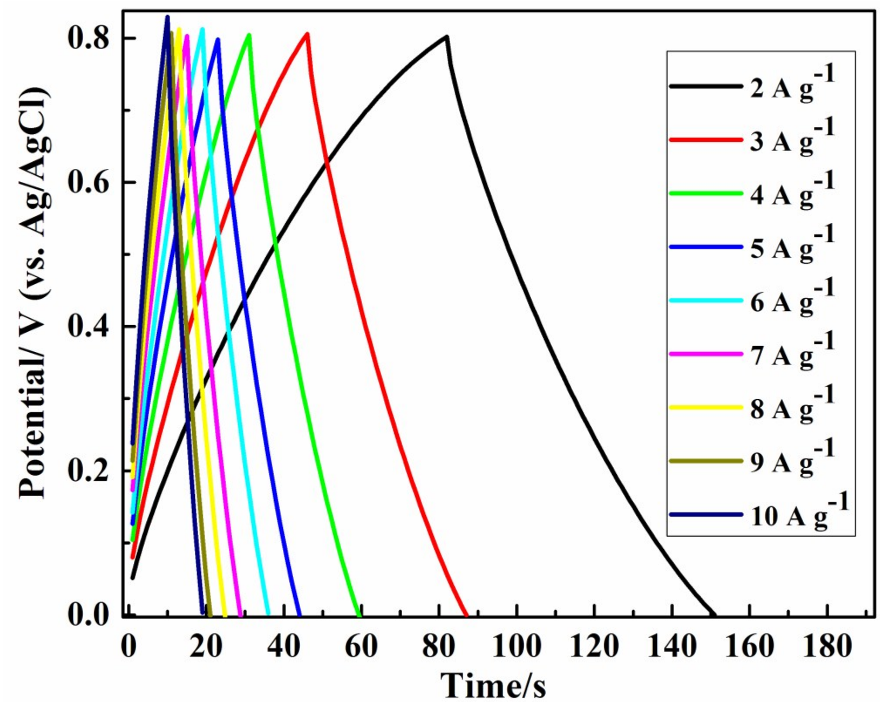

Fig. S10. GCD curves of RGO.

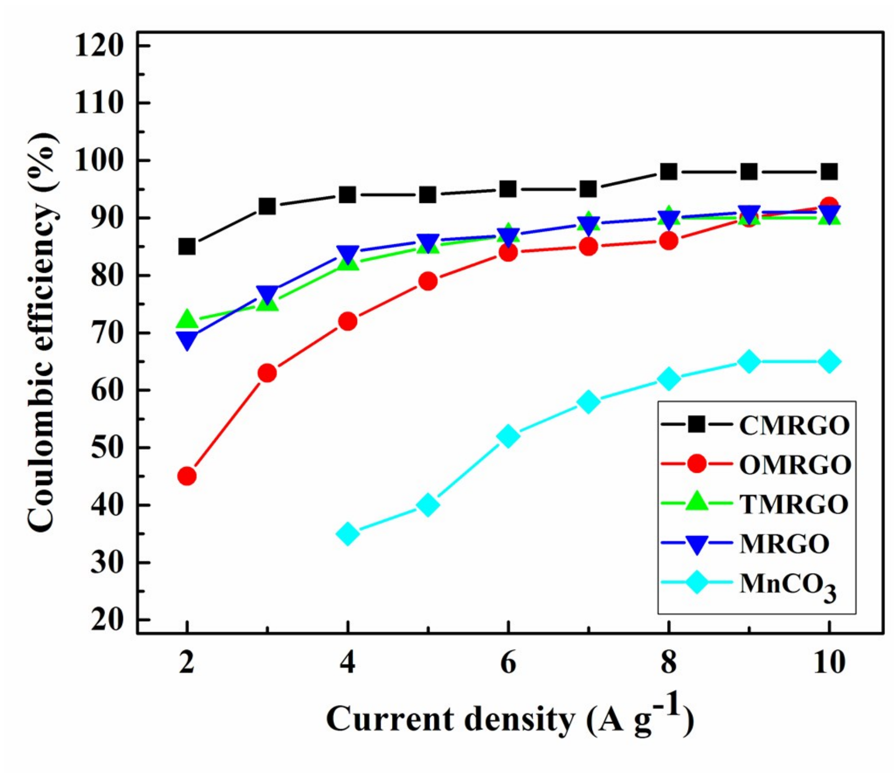

Fig. S11. Coulombic efficiency vs. current density of samples in three electrode configuration.

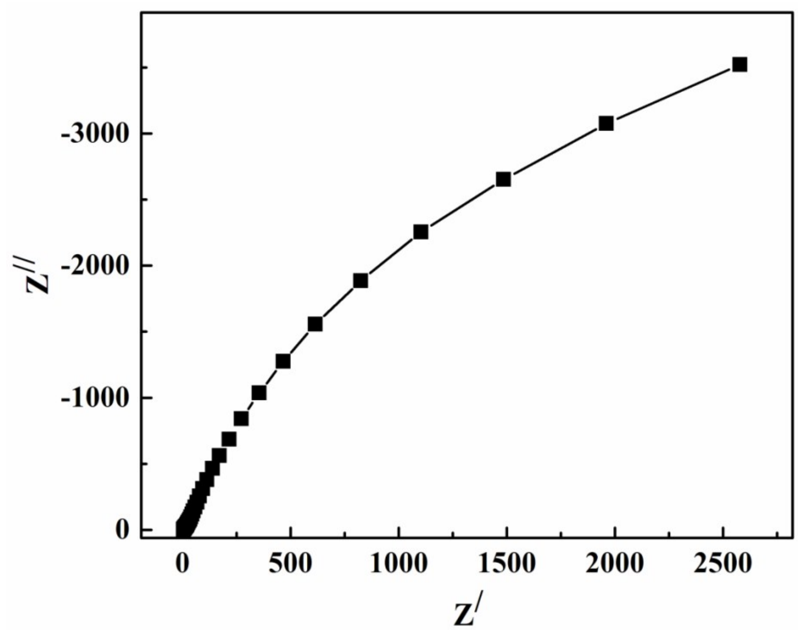

Fig. S12. Nyquist plot of pure $MnCO_3$.

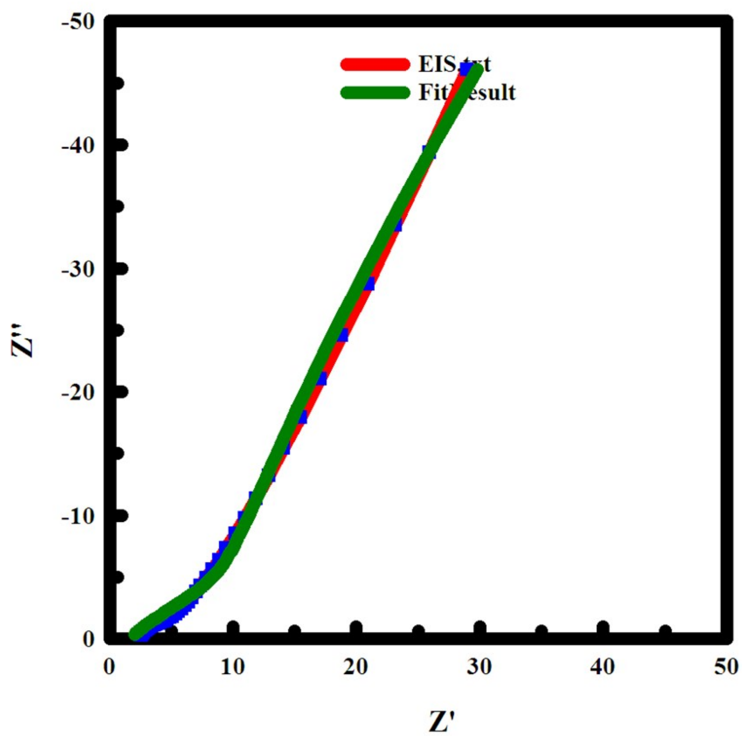

Fig. S13. Z-View fitted Nyquist plot of CMRGO.

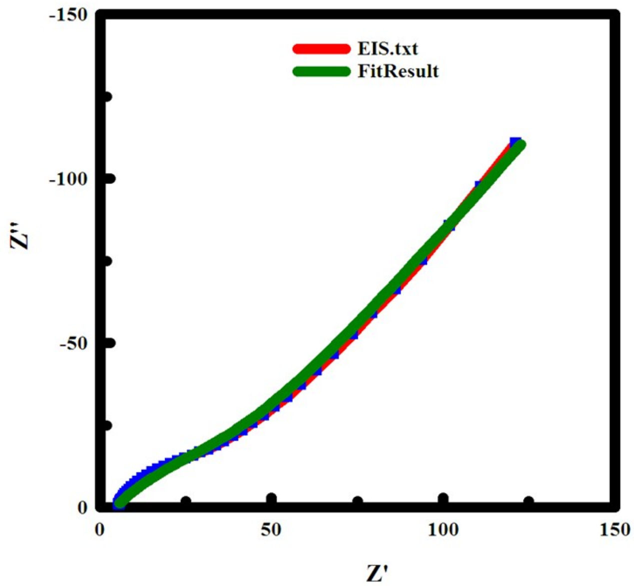

Fig. S14. Z-View fitted Nyquist plot of OMRGO.

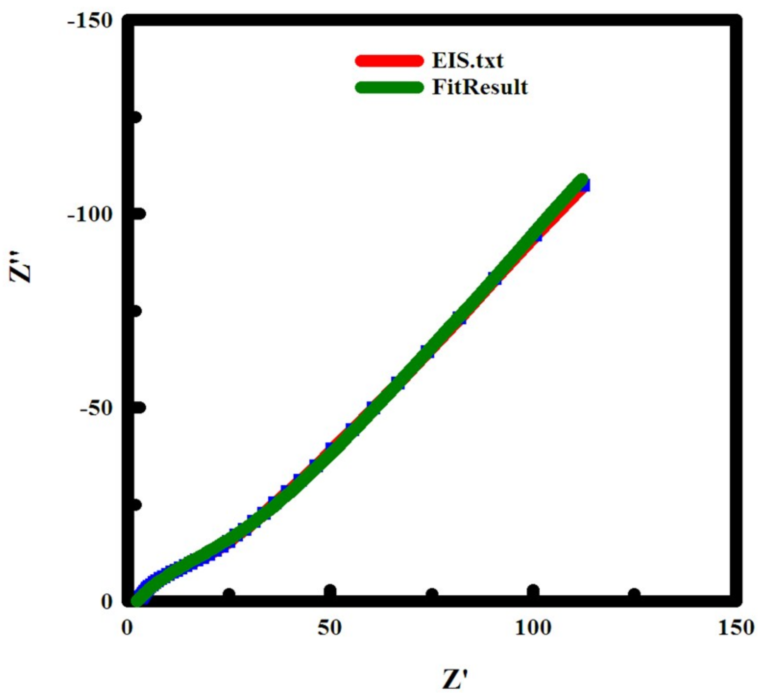

Fig. 15. Z-View fitted Nyquist plot of TMRGO.

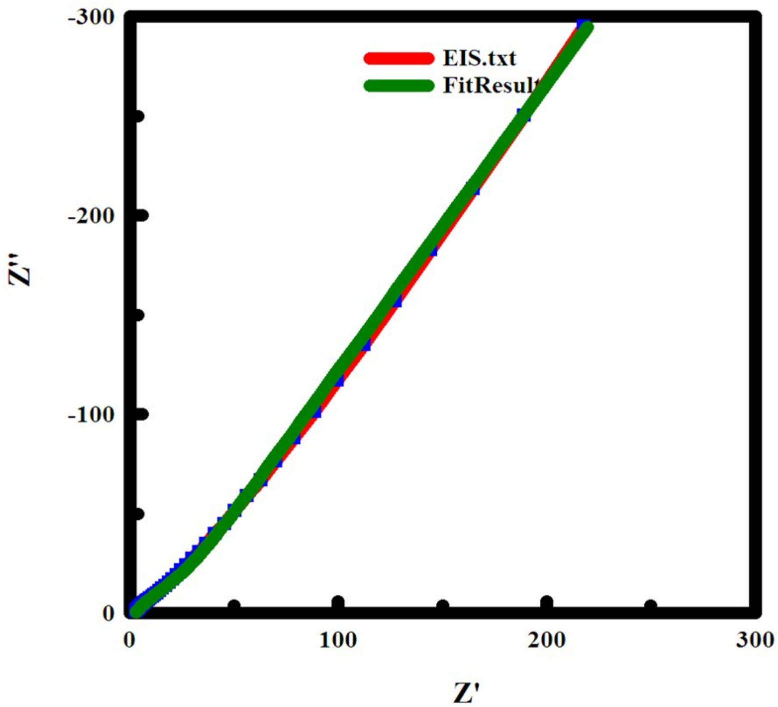

Fig. S16. Z-View fitted Nyquist plot of MRGO.

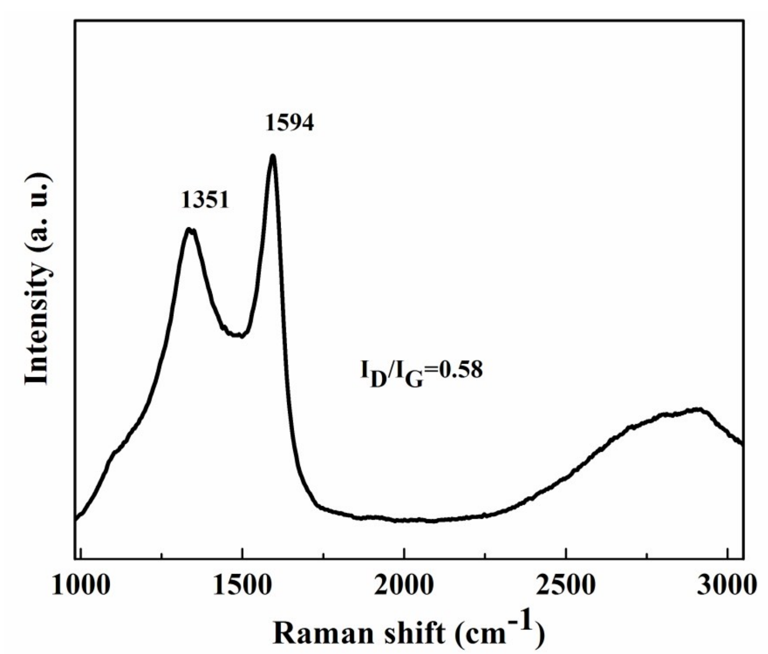

Fig. S17. Raman spectrum of SRGO.

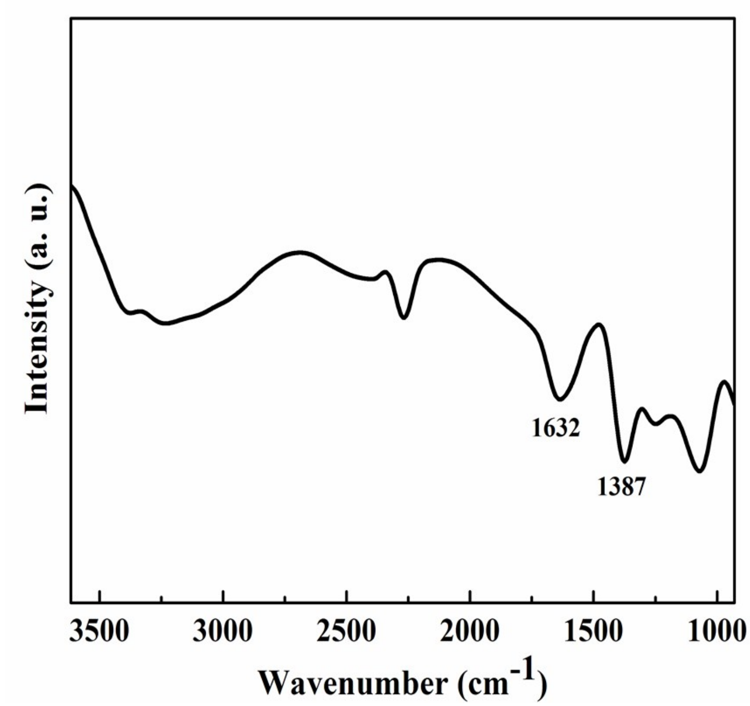

Fig. S18. FT-IR spectrum of SRGO.

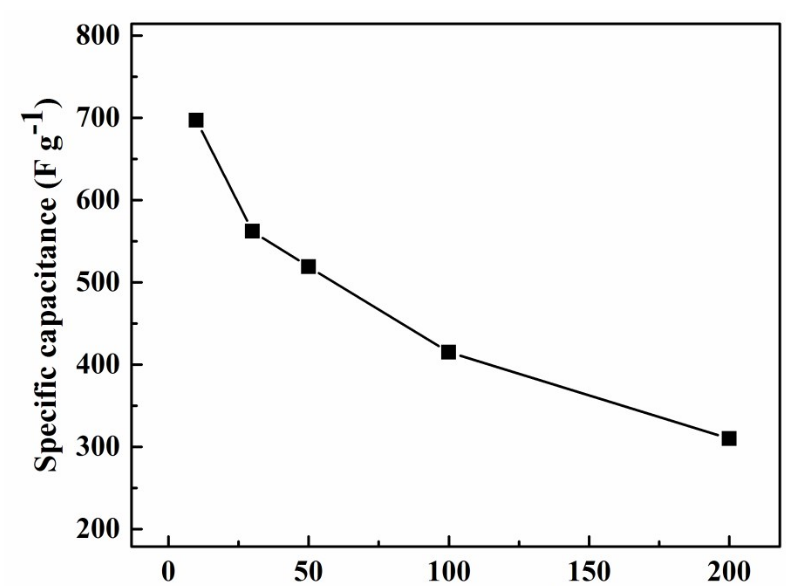

Fig. S19. SC vs. scan rate of SRGO in three electrode configuration.

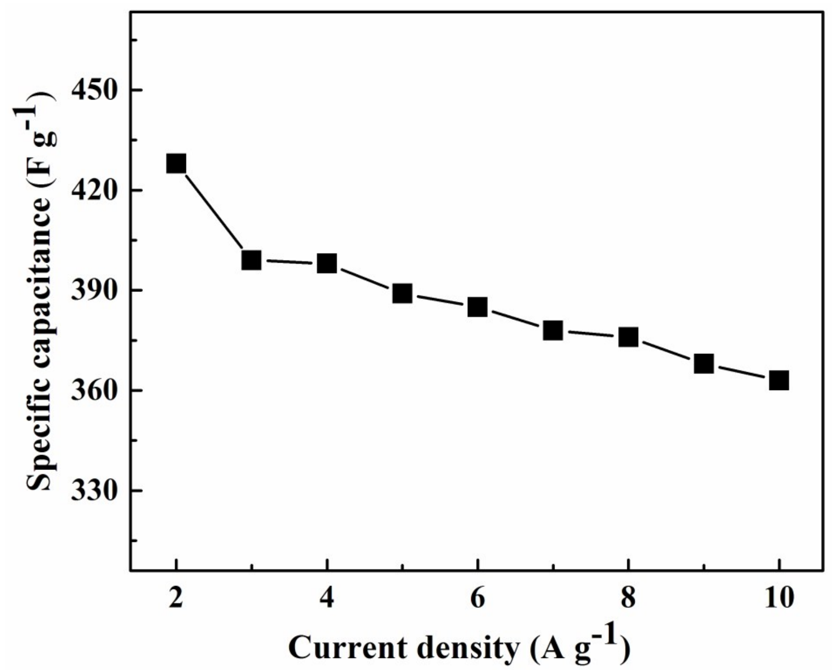

Fig. S20. SC vs. current density of SRGO in three electrode configuration.

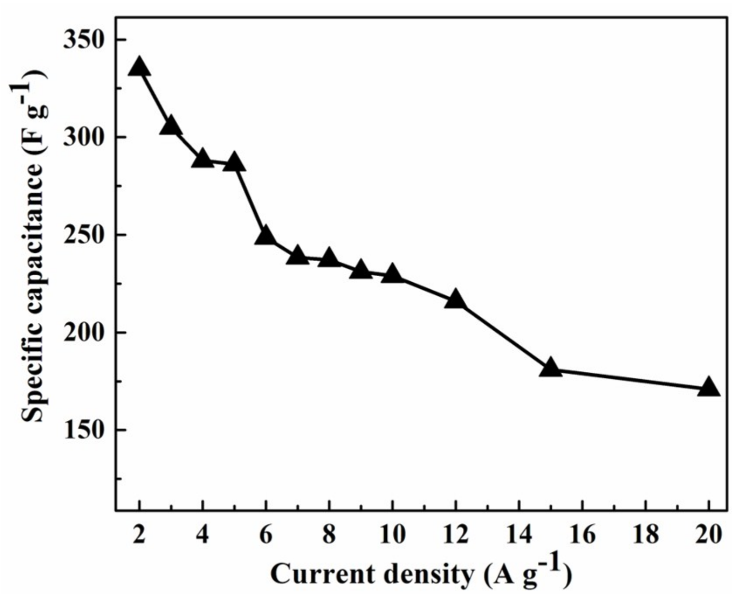

Fig. S21. SC vs. current density plot of ASC.

The areal SC of the ACS based on the area was calculated according to the equation

$$\text{Areal SC} = (I\times\Delta t)/A\times\Delta V \qquad (1).$$

Where, I, A, Δt and ΔV are applied current, area of the device, discharging time and applied potential.

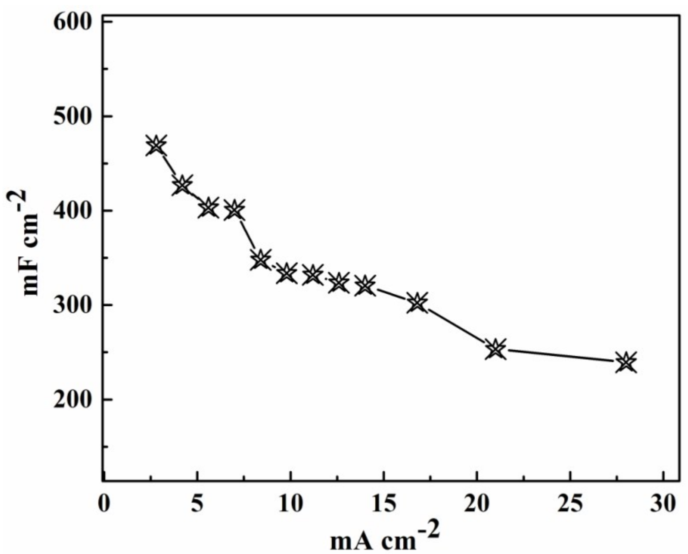

Fig. S22. SC vs. current density plot of ASC according to the area of the ASC.

The volumetric SC of the ACS based on the volume was calculated according to the equation

$$\text{Volumetric SC} = (I\times\Delta t)/v\times\Delta V \qquad (2).$$

Where, I, v, Δt and ΔV are applied current, volume of the device, discharging time and applied potential.

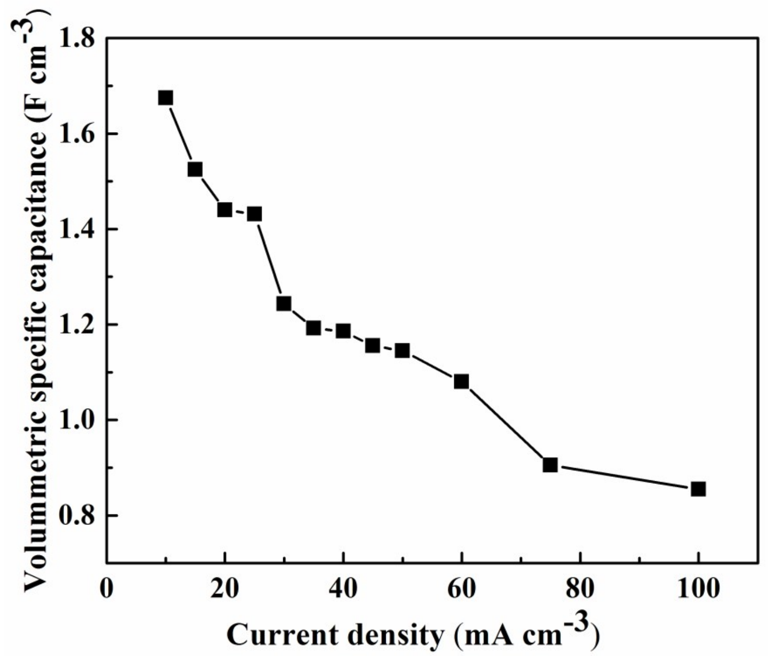

Fig. S23. SC vs. current density plot of ASC according to the volume of the ASC.

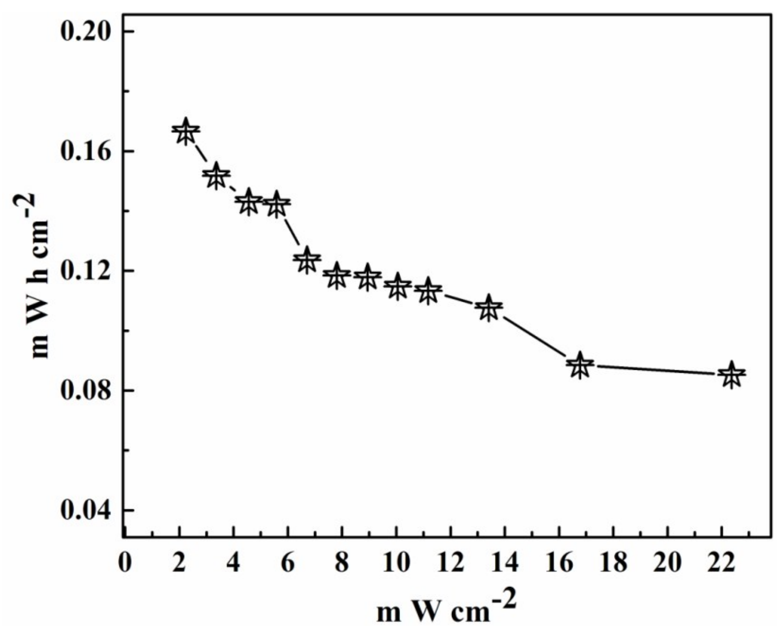

Fig. S24. Areal energy density vs. power density.

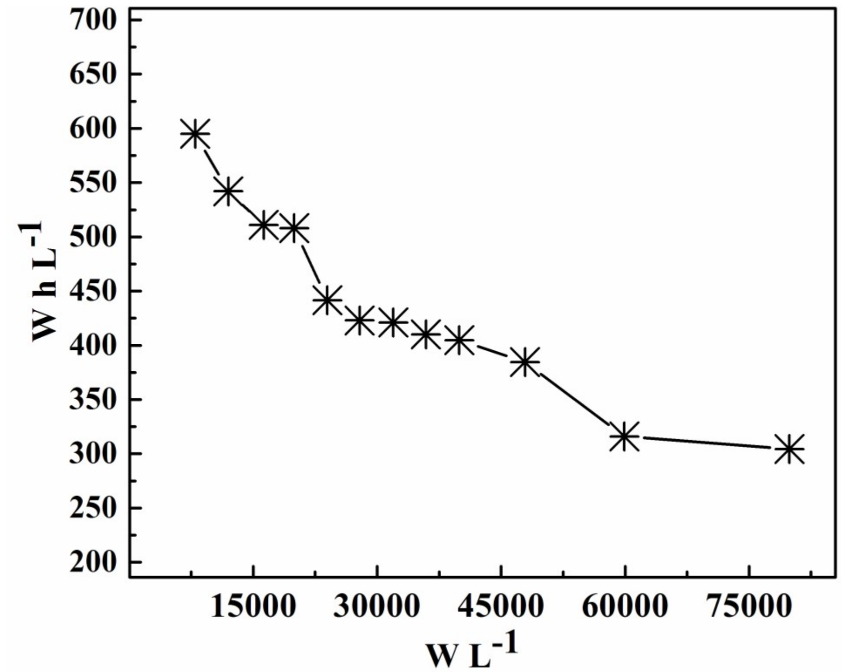

Fig. S25. Volumetric energy density vs. power density.

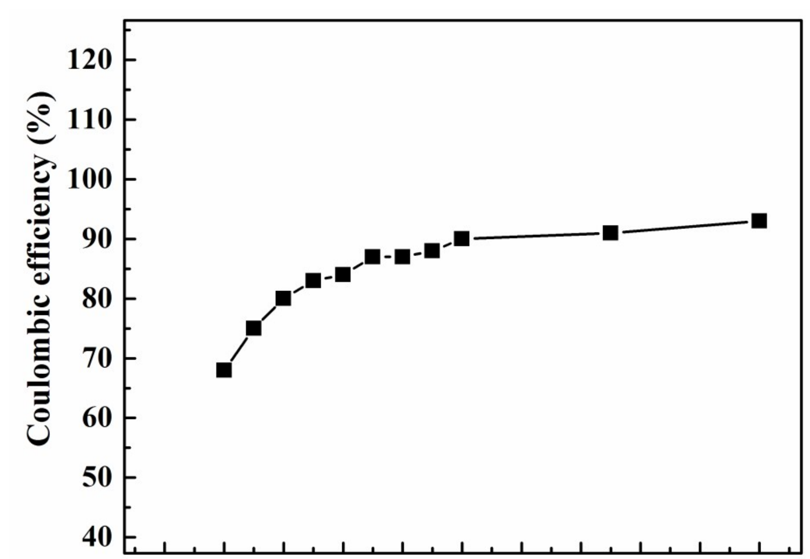

Fig. S26. Coulombic efficiency of ASC at different current densities

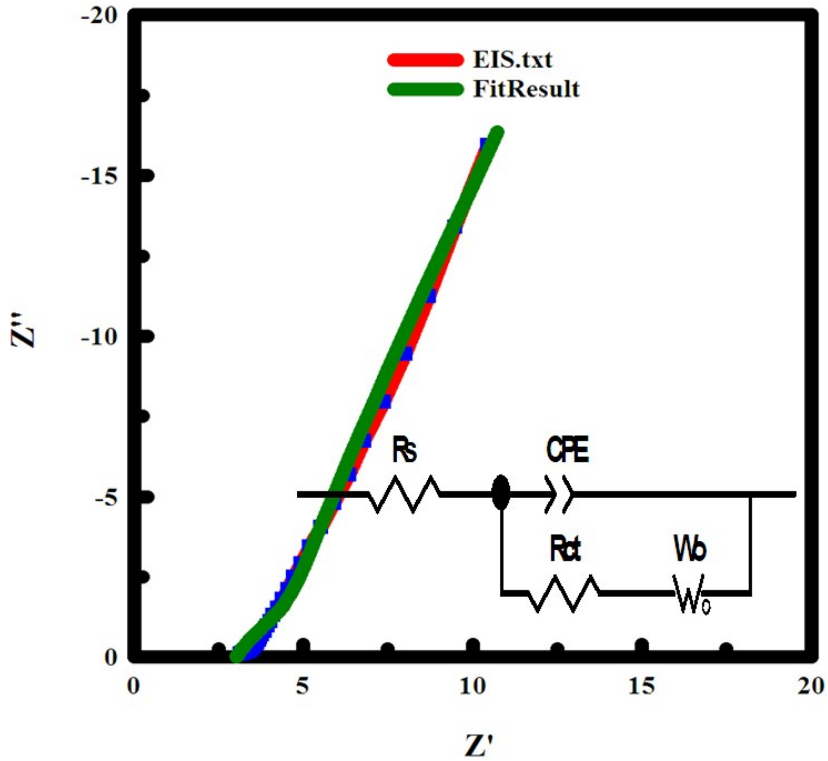

Fig. S27. Z-View fitted Nyquist plot of ASC device.

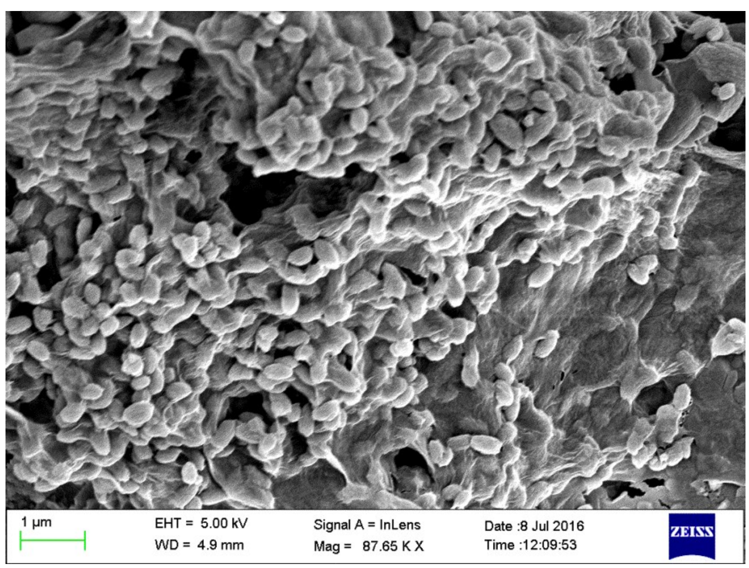

Fig. S28. FE-SEM image of CMRGO after 10,000 GCD cycles.

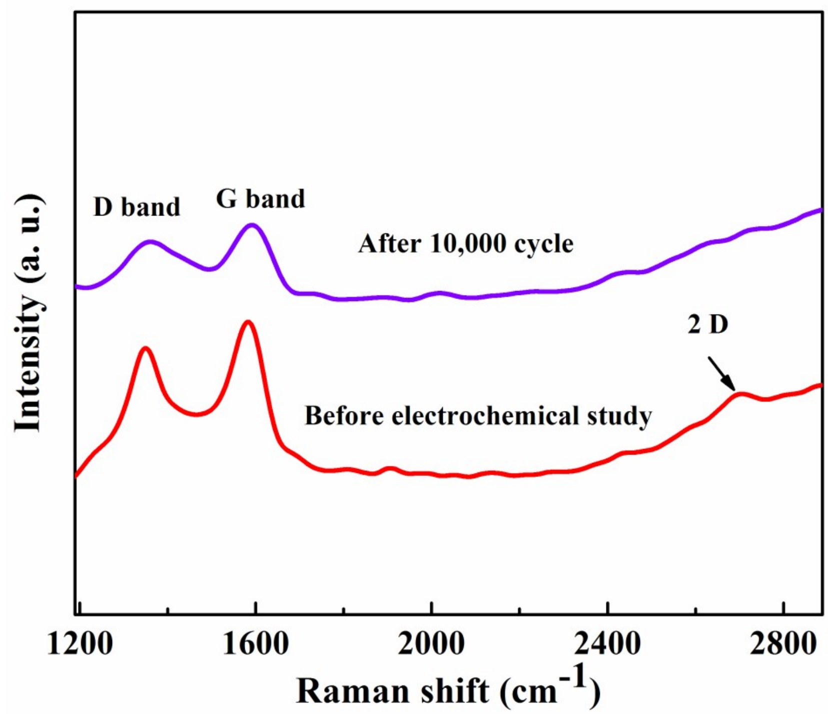

Fig. S29. Raman spectroscopy of CMRGO before and after 10,000 GCD cycles.

Table S1. The comparative supercapacitor performances comparing the mass loading of the active materials with gravimetric energy and power density.

S. N.	Material	SC of 3 electrode (F g^{-1})	Device	Mass loading of device	SC of device	Energy density (W h kg^{-1})	Power density (W kg^{-1})	Reference
1	$NiOOH/Ni_3S_2$/3D Graphene	3296 at 16 A g^{-1}	Ni_3S_2/3D-G//Fe_3O_4/RGO	1.3 mg cm^{-2}	223 F g^{-1} at 5 mV S^{-1} A g^{-1}	82.8	6900	6
2	2D V_2O_5	635 at 1 A g^{-1}	V_2O_5 NS//RGO	0.5 mg cm^{-2}	195 F g^{-1} at 1 A g^{-1}	79.5	900	7
3	RGO/MnO_2	217 F g^{-1} at 100 mA g^{-1}	RGO/MnO_2//RGO	5 mg cm^{-2}	113 mF cm^{-2} at 10 mA g^{-1}	35.1 μ W h cm^{-2}	3.8 mW cm^{-2}	10
4	Functional pillared graphene	388 at 0.5 A g^{-1}	symmetric supercapacitor	2 mg cm^{-2}	61 F cm^{-3} at 0.2 A g^{-1}	18	10000	11
5	Flash Converted Graphene	-----	symmetric supercapacitor	0.49 mg cm^{-2}	88 F g^{-1} at 1 A g^{-1} Or 2.5×10^{-1} F cm^{-3}	9	500000	12
6	Flexible solid-state graphene	-----	symmetric supercapacitor	0.4 mg cm^{-2}	245 F g^{-1} at 1 A g-1	5.87	4.25	13
7	Cobalt hydroxide	1116 at 2 A g^{-1}	Cobalt hydroxide//GO	2.2 mg cm^{-2}	59 F g^{-1} at 6.6 A g-1	11.9 W h kg^{-1}	2540 W kg^{-}	14
8	Co-Al hydroxide nanosheets	1043 F g^{-1} at 1 A g^{-1}	Co-Al hydroxide nanosheets//graphene	2 mg cm^{-2}	-----	20.4 Wh kg^{-1}	9.3 kW kg^{-1}	15
9	$Ni(OH)_2$ nanowire	270 F g^{-1} at 7.5 A g^{-1}	$Ni(OH)_2$//Ordered mesoporous Carbon (wire-shaped micro-supercapacitor)	0.4 mg cm^{-1}	35.67 mF cm^{-2}	0.01 mW h cm^{-2}	7.3 mW cm^{-2}	16
10	Manganosite–microwave exfoliated GO	42.5 ± 9.2 mF cm^{-2}	Manganosite–microwave exfoliated GO//activated carbon	4 mg cm^{-2}	0.11 F cm^{-2}	2.6 W h kg^{-1}	9024 W kg^{-1}	17
11	$MnCO_{3Lotus}$-RGO	1430 F g^{-1} at 2 A g^{-1}	$MnCO_{3Lotus}$-RGO//SRGO	1.4 mg cm^{-2}	335 F g^{-1} at ~2 A g^{-1} or 468 mF cm^{-2} at ~2.8 mA cm^{-2}	120 W h kg^{-1} or 0.16 mW h cm^{-2}	16 kW kg^{-1} or 22 mW cm^{-2}	Present work

Table S2. The comparative supercapacitor performances considering the areal capacitance and volumetric energy and power density.

S. N.	Material	Specific capacitance	Energy density	Power density	Reference
1	MnO_2 porous Nano wires	44.6 mF cm^{-2} at 10 mV s^{-1}	-----	-----	18
2	α-MoO_3 nanoplate/TiO_2 nanotube	43.42 mF cm^{-2} at 20 mV s^{-1}	-----	-----	19
3	Polypyrrole nanobrushes	139 mF cm^{-2}	-----	-----	20
4	Perforated Graphene	67.2 mF cm^{-2}	-----	-----	21
5	3D flexible O/N Co-doped graphene	375 µF cm^{-2} at 1 A g-1	8 W h L^{-1}	8.6 kW L-1	22
6	Triazatruxene	160 mF cm^{-2}	-----	-----	23
7	Graphene	376 F cm^{-3}	13.1 W h L^{-1}	5.9 kW L-1	24
8	Microporous carbon from Pistachio nutshell	29.3 mF cm^{-2}	-----	-----	25
9	Graphene, conducting polymer, and carbon nanotube	52.3 F cm^{-3} at 0.2 A g^{-1}	113 W h L^{-1}	149 kW L^{-1}	26
10	Graphene/Porous Carbon	44 mF cm^{-2}	-----	-----	27
11	Biochar carbon	1.19 F cm^{-2}	-----	-----	28
12	Graphene oxide/polypyrrole/cellulose hybrid	510 mF cm^{-2} at 0.1 mA cm^{-2}	1180 W h L^{-1}	-----	29
13	Polypyrrole (PPy) nanofibers	0.48 mF cm^{-2}	-----	-----	30
14	Fe_2O_3-RGO	11.19 mF cm^{-2}	140 W h L^{-1}	12000 kW L^{-1}	31
15	MnO@C composite	716 mF cm^{-2} at 4 mA cm^{-2}	-----	-----	32
16	Carbon/ TiO_2 micro	27.3 mF cm^{-1} at 0.05 mA cm^{-2}	-----	-----	33
17	Nanostructured copper oxide-painted conductive woven textile	269.2 mF cm^{-2} at 2 mA cm^{-2}	0.082 mW h cm^{-2}	10.1 mW cm^{-2}	34
18	Bi2O3-decorated electrospun carbon nanofibers	530 mF cm-2 at 1 mA cm-2	95 mW h cm^{-2}	11.2 mW cm^{-2}	35
19	carbon fiber bundle@CNT-NiCo(OH)x	-----	840 W h L^{-1}	19.1 kW L^{-1}	36
20	Porous carbon nanosheets	136 mF cm^{-2} at 0.5 mA cm^{-2}	-----	-----	37
21	Nitrogen-doping in carbon cloth	391 mF cm^{-2} at 4 mA cm-2	-----	-----	38

22	WO_3/stainless steel electrode	105 mF cm^{-2} at 5 mV s-	-----	-----	39
23	Present work	468 mF cm^{-2} at 2.8 mA cm-2	0.16 mW h cm^{-2} /594 W h L^{-1}	22 mW cm^{-2}/ 79 kW h L^{-1}	

Mass loading of >1 mg cm^{-2} is generally known as high mass loading for fabricating supercapacitors devices with metal nano particles/ graphene-metal nano particle composites, which provide high SC.[1-5] Plenty of research articles described supercapacitor electrodes with mass loading <1 mg cm^{-2} with high areal SC values.[1-15]

Reference

1. T. Zhai, F. Wang, M. Yu, S. Xie, C. Liang, C. Li, F. Xiao, R. Tang, Q. Wu, X. Lu, and Y. Tong, *Nanoscale*, 2013, **5**, 6790.
2. M. D. Stoller and R. S. Ruoff, *Energy Environ. Sci*., 2010, **3**, 1294.
3. L. Kong, C. Zhang, S. Zhang, J. Wang, R. Cai, C. Lv, W. Qiao, L. Ling, and D. Long, J. *Mater. Chem. A*, 2014, **2**, 17962.
4. Y. Yu, and J. Zhang, *J. Mater. Chem. A*, 2017, **5**, 4719.
5. R. Wang, and X. Yan, *Sci. Rep*., 2014, **4,** 3712.
6. T.-W. Lin, C.-S. Dai, and K. C. Hung, *Sci. Rep*., 2014, **4**, 7274.
7. D. H. Nagaraju, Q. Wang, P. Beaujuge and H. N. Alshareef, *J. Mater. Chem. A*, 2014, **2**, 17146.
8. X. Wang, A. Sumboja, M. Lin, J. Yan, and P. S. Lee, *Nanoscale*, 2012, **4**, 7266.
9. N. Kurra, R. Wang, and H. N. Alshareef, *J. Mater. Chem. A*, 2015, **3**, 7368.
10. A. Sumboja, C. Y. Foo, X. Wang, and P. S. Lee, *Adv. Mater*., 2013, **25**, 2809.
11. L. Jiang, L. Sheng, C. Long, T. Wei and Z. Fan, *Adv. Energy Mater*., 2015, **5**, 1500771.
12. L. J. Wang, M. F. El-Kady, S. Dubin, J. Y. Hwang, Y. Shao, K. Marsh, B. McVerry, M. D. Kowal, M. F. Mousavi and R. B. Kaner, *Adv. Energy Mater*., 2015, **5**, 1500786.
13. P. Du, X. Hu, C. Yi, H. C. Liu, P. Liu, H.-L. Zhang and X. Gong, *Adv. Funct. Mater*., 2015, **25**, 2420.
14. R. R. Salunkhe, B. P. Bastakoti, C.-T. Hsu, N. Suzuki, J. H. Kim, S. X. Dou, C.-C. Hu and Y. Yamauchi, *Chem. Eur. J*., 2014, **20**, 3084.
15. X. Wu, L. Jiang, C. Long, T. Wei and Z. Fan, Adv. Funct. Mater., 2015, 25, 1648.
16. X. Dong, Z. Guo, Y. Song, M. Hou, J. Wang, Y. Wang and Y. Xia, Adv. Funct. Mater., 2014, 24, 3405.
17. D. Antiohos, K. Pingmuang, M. S. Romano, S. Beirne, T. Romeo, P. Aitchison, A. Minett, G. Wallace, and S. Phanichphant, J. Chen, Electrochim. Acta, 2013, 101, 99.

18. J. Song, H. Li, S. Li, H. Zhu, Y. Ge, S. Wang, X. Feng, and Y. Liu, *New J. Chem.*, 2017, 10.1039/C6NJ04118C.
19. S. Sun, X. Liao, Y. Sun, G. Yin, Y. Yao, Z. Huang, and X. Pu, *RSC Adv*., 2017, **7**, 22983.
20. L. M. Santino, S. Acharya, and J. M. D'Arcy, *J. Mater. Chem. A*, 2017, 10.1039/C7TA00369B.
21. R. P. Panmand, P. Patil, Y. Sethi, S. R. Kadam, M. V. Kulkarni, S. W. Gosavi, N. Munirathnam, and B. B. Kale, *Nanoscale*, 2017, **9**, 4801.
22. T. Qin, Z. Wan, Z. Wang, Y. Wen, M. Liu, S. Peng, D. He, J. Hou, F. Huang, G. Cao, *J Power Sources*, 2016, **33**, 455.
23. X.-C. Li, Y. Zhang, C.Y. Wang, Y. Wan, W.-Y. Lai, H. Pang, and W. Huang, *Chem. Sci*., 2017, **8**, 2959.
24. Y. Tao, X. Xie, W. Lv, D.-M. Tang, D. Kong, Z. Huang, H. Nishihara, T. Ishii, B. Li, D. Golberg, F. Kang, T. Kyotani, and Q.-H. Yang, *Sci. Rep*., 2013, **3**, 2975.
25. J. Xu, Q. Gao, Y. Zhang, Y. Tan, W. Tian, L. Zhu, and L. Jiang, *Sci. Rep*., 2014, **4**, 5545.
26. Y. Zhou, N. Lachman, M. Ghaffari, H. Xu, D. Bhattacharya, P. Fattahi, M. R. Abidian, S. Wu, K. K. Gleason, B. L. Wardle, and Q. M. Zhang, *J. Mater. Chem. A*, 2014, **2**, 9964.
27. X. Li , X. Zang, Z. Li, X. Li, P. Li, P. Sun, X. Lee, R. Zhang, Z. Huang, K. Wang, D. Wu, F. Kang, and H. Zhu, *Adv. Funct. Mater*., 2013, **23**, 4862.
28. M. Genovese, and K. Lian, *J. Mater. Chem. A*, 2017, **5**, 3939.
29. Ca. Wan, Y. Jiao, and J. Li, *J. Mater. Chem. A*, 2017, **5**, 3819.
30. C. Shen, C.-P. Wang, M. Sanghadasa, and L. Lina, *RSC Adv*., 2017, **7**, 11724.
31. Q. Lv, K. Chi, Y. Zhang, F. Xiao, J. Xiao, S. Wang, K. P. Loh, *J. Mater. Chem. A*, 2017, **5**, 2759.
32. N. Yu, K. Guo, W. Zhang, X. Wang, and M.-Q. Zhu, *J. Mater. Chem. A*, 2017, **5**, 804.
33. J. Cai, C. Lv, and A. Watanabe, *RSC Adv*., 2017, **7**, 415.
34. S. M. Cha, G. Nagaraju, S. C. Sekhar, and J. S. Yu, *J. Mater. Chem. A*, 2017, **5**, 2224.
35. L. Li, X. Zhang, Z. Zhang, M. Zhang, L.Cong, Y. Pan, and S. Lin, *J. Mater. Chem. A*, 2016, **4**, 16635.
36. X. Lu, Y. Bai, R. Wang, and J. Sun, *J. Mater. Chem. A*, 2016, **4**, 18164.
37. H. Yu, W. Zhang, T. Li, L. Zhi, L. Dang, Z. Liu, and Z. Lei, *RSC Adv*., 2017, **7**, 1067.
38. B. Ouyang, Y. Zhang, Y. Wang, Z. Zhang, H. J. Fan, and R. S. Rawat, *J. Mater. Chem. A*, 2016, **4**, 17801.
39. P. A. Shinde, N. R. Chodankara, V. C. Lokhande, A. M. Patila, T. Jib, J. H. Kim, C. D. Lokhande, *RSC Adv.,* 2016, **6**, 113442.